Progress In Electromagnetics Research M, Vol. 72, 13–21, 2018

The Novel Y Shaped Fractal Defected Ground Structure for the Mutual Coupling Reduction

Yan-Yun Gong*, Ling Wang, and Zhao-Lin Zhang

Abstract—This paper presents a novel Y shaped fractal defected ground structure (FDGS) for the mutual coupling (MC) reduction between coplanar closely spaced microstrip antennas. The proposed FDGS has band-gap characteristic, which induces the current distribution on the antenna patch. This will contribute to achieving 25 dB MC reduction. When realizing the MC reduction, the antenna efficiency is increased. Moreover, the envelope correlation of the MIMO system is decreased, which helps to increase the MIMO system capacity.

1. INTRODUCTION

The mutual coupling (MC) reduction between antenna elements is important in many applications, especially for multiple-input and multiple-output (MIMO) communication systems [1, 2]. The MIMO communication system employs multiple antennas at both the transmitter and receiver, which rely on multiple antennas to offer increases in capacity without the need for additional power or spectrum [3]. However, when the antenna elements in the MIMO communication system are closely spaced, the high MC level between antennas will degrade the antenna performance as well as the MIMO system performance. Therefore, the MC reduction between closely spaced antenna elements in the MIMO communication system is very important in application [4].

The MC reduction between the closely spaced antennas is difficult to achieve [5–7]. By etching the elliptical split-ring resonators placed horizontally between the antennas, the 19 dB MC reduction between two closely spaced antennas with center-to-center distance $0.25\lambda_0$ is achieved in [8]. An efficient technique based on a T-shaped slot is introduced in [9] to reduce the MC between closely spaced PIFAs (Planar Inverted-F Antennas) for MIMO mobile terminals, and the isolation of above 40 dB is realized. The isolation of more than 36.5 dB is achieved by a slot on the ground plane [10], which operates at 2.4 GHz with an inter-PIFA spacing of center-to-center distance $0.063\lambda_0$. By the etched slot structure in a ground plane [11], the isolation of more than 20 dB is achieved between two parallel PIFAs with center-to-center $0.115\lambda_0$. A dumb-bell-like DGS reducing the MC between closely-packed antennas is proposed in [12], and the 18 dB MC reduction is achieved between antennas with center-to-center distance $0.45\lambda_0$.

Except for the MC reduction between PIFAs, approaches for the MC reduction between closely placed microstrip antennas also have been studied. The designs of the folded split-ring resonators etched in the ground plane are proposed for the MC reduction between microstrip antennas [13]. A reduction of more than 30 dB MC between microstrip antennas with a very close distance $0.27\lambda_0$ (center-to-center) is obtained. The microstrip antennas loaded with the coupled split ring resonators are presented in [14], and about 10 dB MC reduction is realized of the antenna elements in the case of $0.27\lambda_0$ inter-element spacing. By inserting the band-gap waveguided metamaterials between two microstrip antennas with the center-to-center distance $0.35\lambda_0$, about 6 dB MC reduction is achieved [15]. A novel miniaturized

Received 23 June 2018, Accepted 26 July 2018, Scheduled 13 August 2018
* Corresponding author: Yan-Yun Gong (yanyun_gong@mail.nwpu.edu.cn).
The authors are with the School of Electronics and Informatics, Northwestern Polytechnical University, Xi'an 710072, P. R. China.

two-layer electromagnetic band-gap (EBG) structure is presented in [16] for reducing the MC between closely spaced (center-to-center distance $0.3\lambda_0$) planar printed antennas on a common ground, and more than 10 dB MC reduction across the operating band is achieved. An asymmetrical coplanar strip wall suppresses the MC between two closely spaced microstrip antennas [17], and the achieved isolation is better than 35 dB. A hybrid solution is proposed in [18] to achieve the 20 dB MC reduction between closely spaced microstrip antennas (center-to-center distance is $0.28\lambda_0$), which is realized by a metallic wall combined with two open-ended slots. An H-shaped conducting wall that effectively suppresses the 25 dB MC between two closely spaced microstrip antennas, which has center-to-center distance of $0.34\lambda_0$, is introduced in [19].

When designing a planar band-gap structure filter, the minimization of circuit dimension is required for the closely spaced elements of antenna array. A Koch fractal based DGS is used to reduce the MC between two closely spaced (center-to-center distance $0.29\lambda_0$) planer monopole patch antennas, and 15 dB MC reduction is obtained [20]. A Minkowski fractal DGS is proposed to obtain 7 dB MC reduction in a compact monopole array with center-to-center distance $0.1\lambda_0$ [21]. The EBG for mutual coupling reduction between dual-element MIMO antennas is presented in [22]. It gives 19 dB and 11 dB simulated mutual coupling reductions in E-plane and H-plane, respectively. The comparisons of the MC reduction method and their performance are summarized in the Table 1.

Table 1. Comparison of the mutual coupling reduction method and their performance.

	Antenna type	Decoupling structure	center-to-center	edge-to-edge	MC reduction
Ref. [13]	Microstrip antenna	Split-ring resonators DGS	$0.27\lambda_0$	$0.039\lambda_0$	30 dB
Ref. [14]	Microstrip antenna	Split-ring resonators wall	$0.27\lambda_0$	$0.12\lambda_0$	10 dB
Ref. [15]	Microstrip antenna	Waveguided metamaterial	$0.35\lambda_0$	$0.125\lambda_0$	6 dB
Ref. [16]	Microstrip antenna	EBG	$0.3\lambda_0$	$0.15\lambda_0$	10 dB
Ref. [17]	Microstrip antenna	Coplanar strip wall	$0.28\lambda_0$	$0.03\lambda_0$	35 dB
Ref. [18]	Microstrip antenna	Metallic wall	$0.28\lambda_0$	$0.03\lambda_0$	20 dB
Ref. [19]	Microstrip antenna	Conducting wall	$0.34\lambda_0$	$0.052\lambda_0$	25 dB
Ref. [22]	Microstrip antenna	EBG	$0.22\ \lambda_0$	$0.14\ \lambda_0$	19 dB
proposed	Microstrip antenna	Fractal DGS	$0.20\lambda_0$	$0.048\lambda_0$	25 dB

A Y-shaped fractal defected ground structure (FDGS) for the MC reduction between closely spaced microstrip antennas in a MIMO wireless communication system is proposed in this paper. The center-to-center distance between the closely placed microstrip antennas is $0.2\lambda_0$. The decoupling FDGS is etched between microstrip antennas and achieves 25 dB MC reduction. When realizing the MC reduction, the antenna performance is improved, and the microstrip antenna keeps a low profile at the same time.

This paper is organized as follows. The structure of the proposed FDGS geometry and its MC reduction are analyzed in Section 2. The simulation and measurement results are indicated in Section 3. The conclusion is given in Section 4.

2. FDGS GEOMETRY AND CHARACTERISTIC

2.1. FDGS Structure

The geometries of the designed fractal of zero, first, second and third iterative structures are drawn in Fig. 1. The zero iterative structure is a straight line as shown in Fig. 1(a). By folding the straight line to Y-shaped structure as shown in Fig. 1(b), the first iterative fractal structure is designed. The first iterative fractal structure is regarded as the basic fractal unit. As shown in Fig. 1(c), the second iterative structure is evolved from the first iterative structure by turning two line-segments into two basic fractal units. The third iterative fractal structure is evolved from the second iterative fractal structure as shown in Fig. 1(d) by turning four line-segments of the second iterative fractal structure to four basic fractal units. By repeating this process, the high level iterative fractal structure is designed.

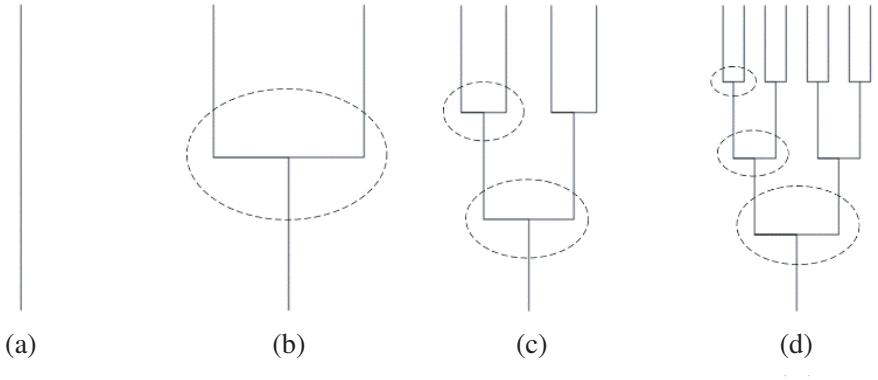

Figure 1. Design of the fractal geometries; (a) zero iteration, (b) first iteration, (c) second iteration, (d) third iteration.

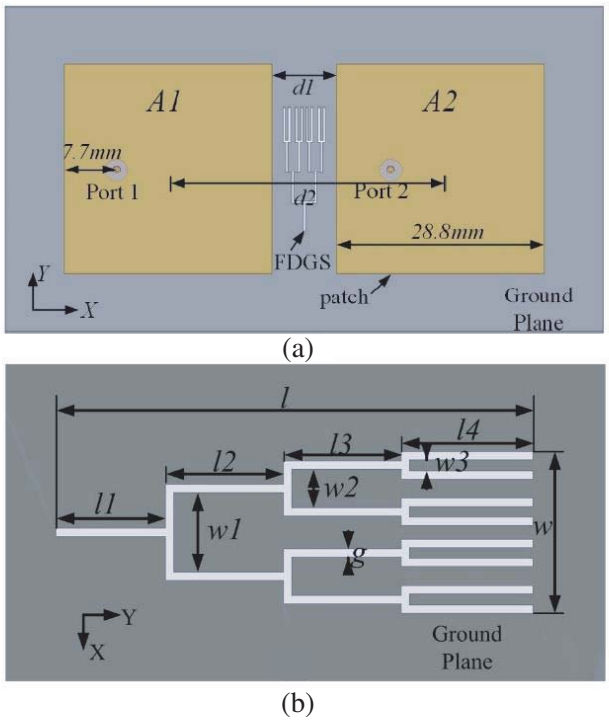

Figure 2. Geometry of the (a) proposed microstrip antenna array with the FDGS in the ground plane, (b) the third iterative FDGS.

The model of the third iterative FDGS and the microstrip antennas in a MIMO wireless communication system are shown in Fig. 2. Two horizontally polarized microstrip antennas are placed along the x-axis. Both the antenna elements have the same resonant band with center frequency 1.57 GHz. The chosen substrate is Taconic CER-10 with dielectric constant 10, height 3.18 mm and loss tangent 0.0035. The dimension of the rectangular patch is $28.8 \times 28.8\,\text{mm}^2$. The pair of microstrip antennas has the center-to-center distance of $d2 = 38\,\text{mm}$ ($0.2\lambda_0$, where λ is the free space wavelength at 1.57 GHz) and the edge-to-edge distance of $d1 = 9.2\,\text{mm}$ ($0.048\lambda_0$). The rectangular patch dimension is $28.8 \times 28.8\,\text{mm}^2$.

2.2. FDGS Mutual Coupling Reduction Characteristic

In order to obtain better MC reduction performance by the proposed FDGS, the model of the FDGS and the microstrip antennas are optimized using the Ansoft HFSS (High Frequency Structure Simulator). The optimized parameter values are: $l = 17.1\,\text{mm}$, $w = 5.9\,\text{mm}$, $l1 = 4\,\text{mm}$, $l2 = 4.3\,\text{mm}$, $l3 = 4.3\,\text{mm}$, $l4 = 4.5\,\text{mm}$, $w1 = 2.9\,\text{mm}$, $w2 = 1.4\,\text{mm}$, $w3 = 0.4\,\text{mm}$, $g = 0.3\,\text{mm}$.

The proposed Y-shaped FDGS provides rejection band in some frequency range, which achieves the MC reduction between antenna elements. The FDGS structure is etched away from the ground plane, and a transmission line is placed on a vacuum box above the ground plane. The transmission line has a strip width 1.2 mm and length 45 mm. There are two ports connecting the end of the transmission line. The center working frequency of the proposed FDGS is $f0$. The return loss and transmission coefficient of the transmission line are drawn in Fig. 3. Band-gap characteristic is reflected on the S_{12}, where the

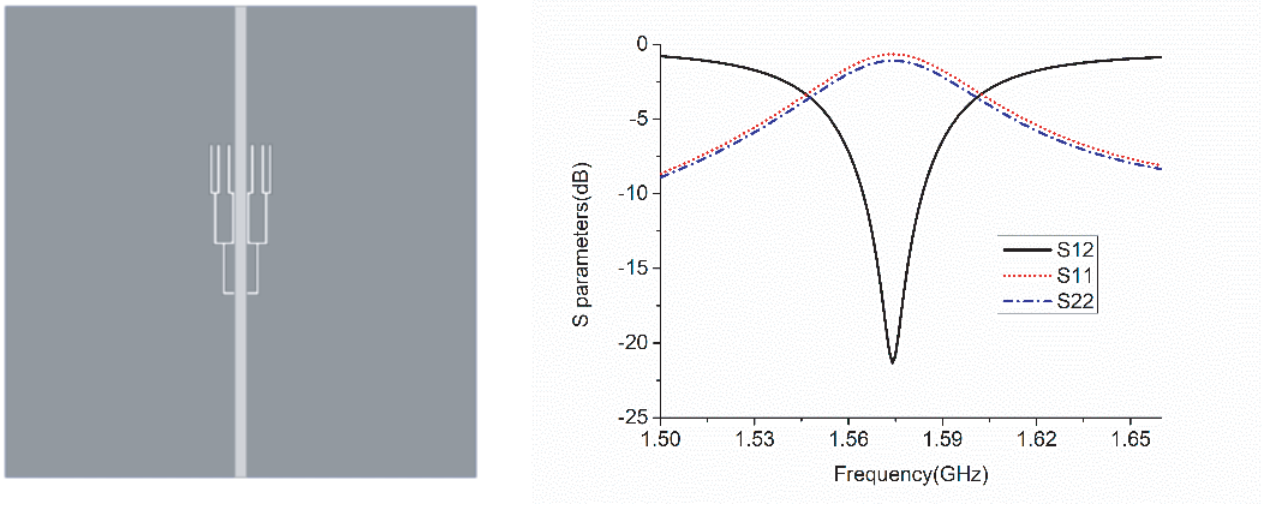

Figure 3. S parameters of designed third iterative FDGS band-gap filter.

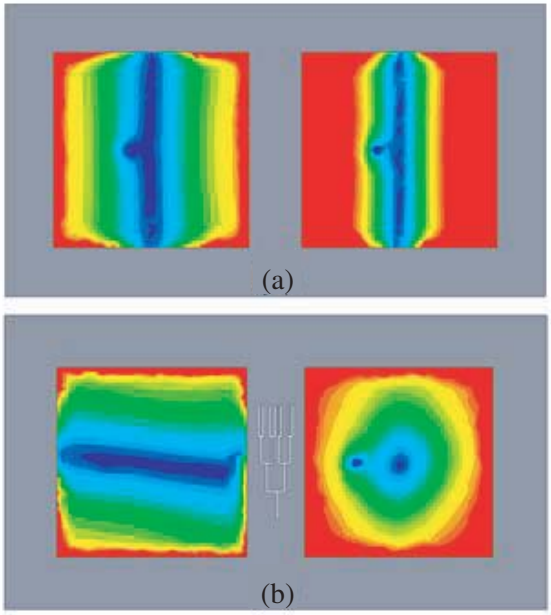

Figure 4. The current distributions on the antenna patches with and without the proposed FDGS.

resonant frequency $f0$ is 1.57 GHz.

Supposing that the right positioned antenna *A2* is excited and that the left positioned antenna *A1* is terminated with a 50 Ω load, the current distributions on the antenna patches with and without the proposed FDGS are shown in Fig. 4. When the microstrip antennas are placed on a ground plane without FDGS, a large current distribution is detected on the radiated patches. The large current distribution causes a high MC level between the antenna elements. When the proposed FDGS is etched from the ground plane, the suppressed current distribution is detected on the radiated patches. It means that the proposed Y-shaped FDGS induces the current fields and suppresses the current distribution on the antenna patches, which explains the MC reduction achieved by this proposed method.

The mutual coupling reduction performance of the proposed FDGS is evaluated from the S_{12} corresponding to different FDGS dimensions. Fig. 5 shows the S_{12} of antenna array with deferent FDGS lengths l (only $l4$ is from 4 mm to 5 mm with step 0.5 mm). When the proposed FDGS gap length increases, the MC reduction working band moves to the lower frequency region. We can get the same conclusion when tuning the other slot length $l1$, $l2$ and $l3$. Fig. 6 illustrates the S_{12} between antennas when the gap width g ranges from 0.3 mm to 0.4 mm with step 0.05 mm. As the etched gap width increases, the operative MC reduction working band moves up to higher frequency. In general, the increased slot length and decreased slot width give rise to lower cutoff frequency.

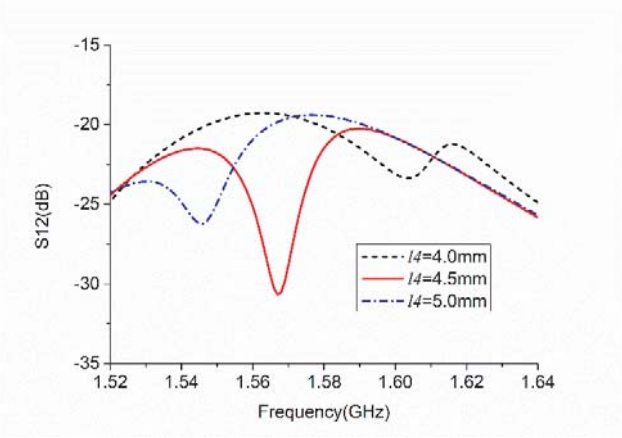

Figure 5. The S_{12} between the antennas when tuning the FDGS slot length.

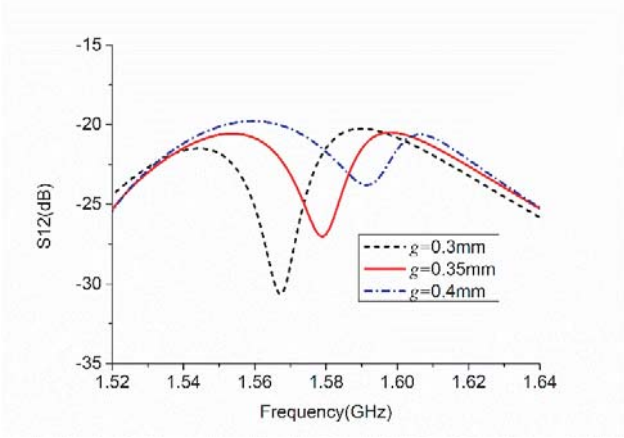

Figure 6. The S_{12} between the antennas when tuning the FDGS slot width.

2.3. The Optimized Simulation Results

The return loss and mutual coupling of the antenna elements with and without the proposed Y-shaped FDGS are plotted in Fig. 7. The S_{12} comparison of the microstrip antenna arrays with and without the FDGS shows that the MC level is reduced from −5 dB to −30 dB. About 25 dB MC reduction between antenna elements is achieved. Furthermore, the S_{12} value is less than −20 dB within the antenna 10-dB impedance bandwidth. It is shown that the working frequency of the antenna element shifts 10 MHz to the high frequency region by the FDGS. Because the antenna resonant band can be shifted by adjusting the patch dimension, the proposed FDGS is valid and efficient in application.

The envelope correlation between antenna elements is one of the most important parameters because it is related with antenna efficiency and may degrade MIMO system performance. Research has shown that the envelope correlation can be defined by one simple equation correlated to the scattering parameters of the elements in antenna array. For two antenna elements, the envelope correlation equation using the scattering parameters is given by:

$$\rho_e = \frac{\left|S_{11}^* S_{12} + S_{21}^* S_{22}\right|^2}{\left(1 - \left|S_{11}\right|^2 - \left|S_{21}\right|^2\right)\left(1 - \left|S_{22}\right|^2 - \left|S_{12}\right|^2\right)}$$

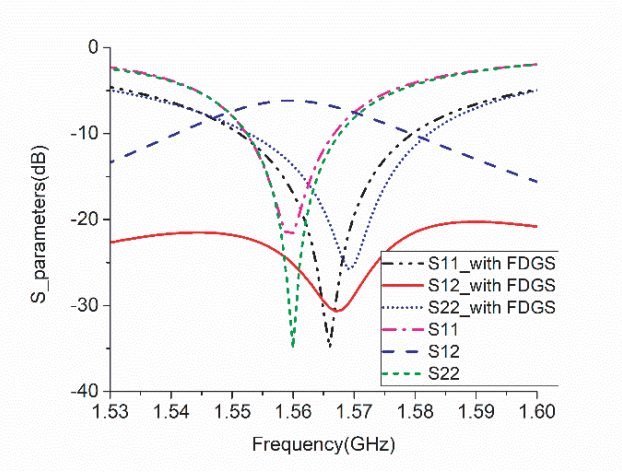

Figure 7. S parameters of antenna array with proposed FDGS.

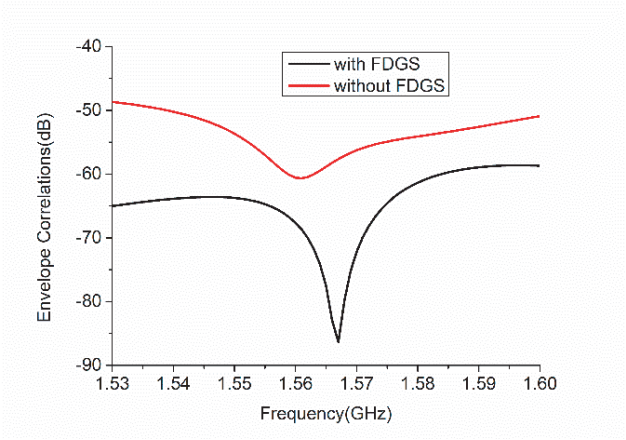

Figure 8. Envelope correlation of antenna array with and without FDGS.

For illustrating the benefits achieved by the proposed FDGS, the envelope correlation of the antenna array in a MIMO system is calculated. In Fig. 8, the envelope correlations against frequency for the MIMO system with and without the proposed FDGS are plotted. From the simulation result, the envelope correlation value of the MIMO system with the FDGS is decreased compared to that of the MIMO system without the FDGS. The envelope correlation suppression will contribute to increase of the MIMO system capacity. This observation indicates a better behavior and performance of the MIMO system which will be achieved by the proposed Y-shaped FDGS.

Antenna main polarization radiation patterns on the E-plane and H-plane with and without the proposed Y-shaped FDGS are depicted in Figs. 9(a) and (b), respectively, when antenna *A2* is excited and antenna *A1* terminated with a 50 Ω load. The back lobe levels with the FDGS are greater than that without the FDGS on both E-plane and H-plane because of slots on the ground plane. Radiation pattern on the E-plane is more symmetrical in the upper-sphere space by using the proposed FDGS. No significant difference is found between the main polarization radiation patterns with and without the FDGS in the H-plane. When realizing the MC reduction, the antenna efficiency is improved from 76.1% to 82.4%.

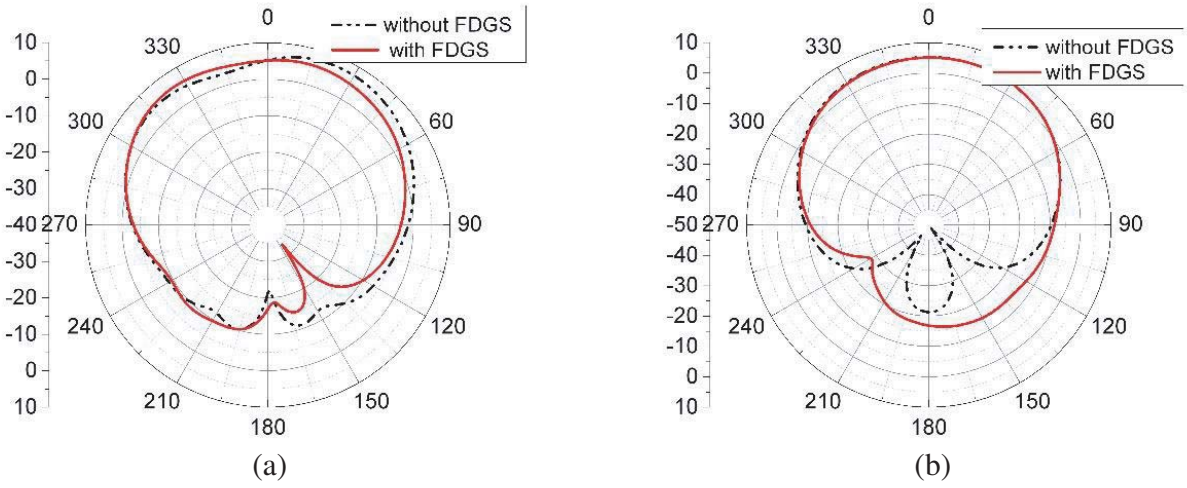

Figure 9. Far-field radiation patterns with and without FDGS at center frequency. (a) E-plane. (b) H-plane.

3. THE SIMULATION AND MEASUREMENT RESULTS

In order to validate the MC reduction performance by the proposed Y-shaped FDGS, the prototype is fabricated based on the optimized parameters, as shown in Fig. 10. The S-parameter of the fabricated antennas is measured by the Agilent E5230A network analyzer.

Figure 10. The fabricated antenna array with the Y shaped FDGS.

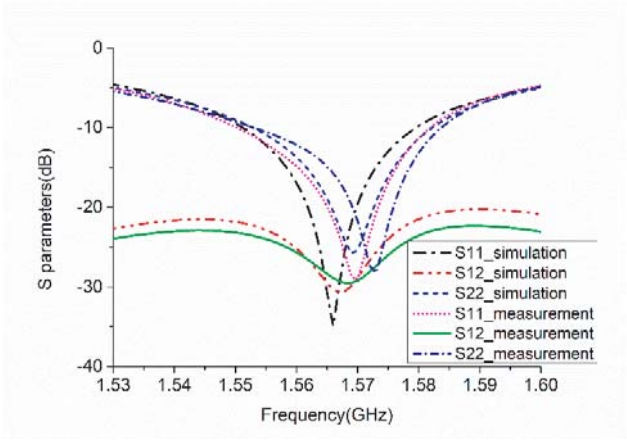

Figure 11. The simulated and measured S parameters with the FDGS.

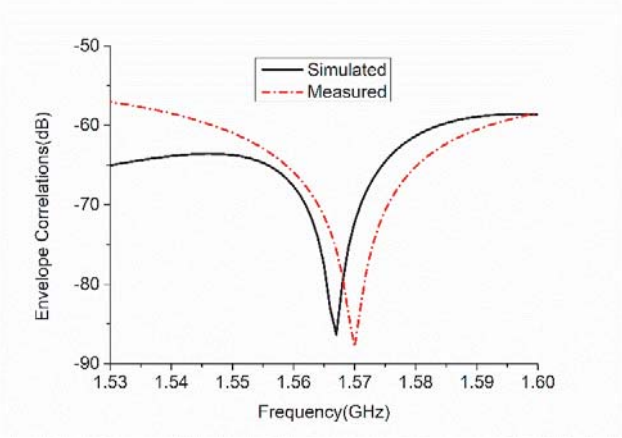

Figure 12. The simulated and measured envelope correlations with the FDGS.

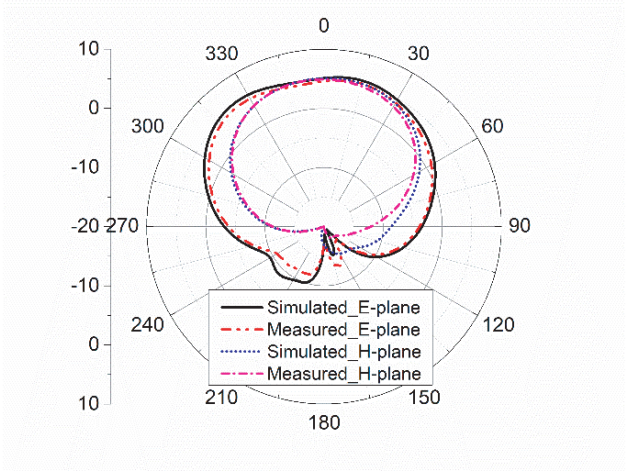

Figure 13. The simulated and measured radiation patterns on E-plane and H-plane.

The simulated and measured S parameters of the microstrip antennas are plotted in Fig. 11. The simulated and measured S_{12} coincide with each other, which indicates the good simulation and measurement agreement. S_{12} is less than -30 dB at the center frequency, and 25 dB MC reduction between antennas elements is obtained in both the simulation and measurement. Note that the measured S-parameters shifts a little to the higher frequency region. These differences between simulation and measurement are mainly caused by the machine error of the fabricated antenna and the FDGS dimension.

The simulated and measured envelope correlations with the FDGS are plotted in Fig. 12 for comparison. Both the results are calculated by the formula in Section 2. The simulation and measurement results are coincident with each other, which indicates that the envelope correlation

suppression is obtained. The decreased envelope correlation in the MIMO antenna array will contribute to increase of the MIMO system capacity.

The simulated and measured main polarization radiation patterns of the right positioned antenna element *A2* on the *E*-plane and *H*-plane with the FDGS are illustrated in Fig. 13, when the antenna element *A2* is excited and element *A1* terminated with a 50 Ω load. Measurement results coincide with the simulated ones. There is no significant difference between the simulated and measured main lobe patterns.

4. CONCLUSION

A Y-shaped FDGS is proposed in this paper for the MC reduction between closely placed microstrip antennas in a MIMO system. The proposed Y-shaped FDGS suppresses the current distribution on the antenna patch, which explains the MC reduction achieved by this proposed method. Approximately 25 dB MC reduction between two coplanar microstrip antennas is obtained. When realizing the MC reduction, the antenna efficiency is improved from 76.1% to 82.4%. Moreover, the envelope correlation of the MIMO system with the FDGS is decreased when achieving the MC reduction, which will contribute to increase of the MIMO system capacity.

ACKNOWLEDGMENT

This study was supported in part by the National Natural Science Foundation of China (Nos. 61771404, 61601372, and 61301093).

REFERENCES

1. Fletcher, P. N., M. Dean, and A. R. Nix, "Mutual coupling in multi element array antennas and its influence on MIMO channel capacity," *Electron. Lett.*, Vol. 39, No. 4, 342–344, 2003.
2. Getu, B. N. and R. Janaswamy, "The effect of mutual coupling on the capacity of the MIMO cube," *IEEE Antennas Wireless Propag. Lett.*, Vol. 4, 240–244, 2005.
3. Lu, S., T. Hui, and M. Bialkowski, "Optimizing MIMO channel capacities under the influence of antenna mutual coupling," *IEEE Antennas Wireless Propag. Lett.*, Vol. 7, 287–290, 2008.
4. Ludwig, A., "Mutual coupling, gain and directivity of an array of two identical antennas," *IEEE Trans. Antennas Propag.*, Vol. 24, No. 6, 837–841, Nov. 1976.
5. Zhang, S., A. A. Glazunov, Z. Ying, and S. He, "Reduction of the envelope correlation coefficient with improved total efficiency for mobile LTE MIMO antenna arrays: Mutual scattering mode," *IEEE Trans. Antennas Propag.*, Vol. 61, No. 6, 3280–3291, 2013.
6. Li, H., J. Xiong, and S. He, "A compact planar MIMO antenna system of four elements with similar radiation characteristics and isolation structure," *IEEE Antennas Wireless Propag. Lett.*, Vol. 8, 1107–1110, 2009.
7. Ibrahim, A. A., M. A. Abdalla, A. B. Abdel-rahman, and H. F. A. Hamed, "Compact MIMO antenna with optimized mutual coupling reduction using DGS," *International Journal of Microwave and Wireless Technologies*, Vol. 6, No. 2, 173–180, 2014.
8. Hafezifard, R., M. Naser-Moghadasi, J. R. Mohassel, and R. A. Sadeghzadeh, "Mutual coupling reduction for two closely spaced meander line antennas using metamaterial substrate," *IEEE Antennas Wireless Propag. Lett.*, Vol. 15, 40–43, 2016.
9. Zhang, S., B. K. Lau, Y. Tan, Z. Ying, and S. L. He, "Mutual coupling reduction of two PIFAs with a T-shape slot impedance transformer for MIMO mobile terminals," *IEEE Trans. Antennas Propag.*, Vol. 60, No. 3, 1521–1531, 2012.
10. Zhang, S., S. N. Khan, and S. L. He, "Reducing mutual coupling for an extremely closely-packed tunable dual-element PIFA array through a resonant slot antenna formed in-between," *IEEE Trans. Antennas Propag.*, Vol. 58, No. 8, 2771–2776, 2010.

11. Chiu, C. Y., C. H. Cheng, R. D. Murch, and C. R. Rowell, "Reduction of mutual coupling between closely-packed antenna elements," *IEEE Trans. Antennas Propag.*, Vol. 55, No. 6, 1732–1738, 2007.
12. Zhu, F. G., J. D. Xu, and Q. Xu, "Reduction of mutual coupling between closely-packed antenna elements using defected ground structure," *Electron. Lett.*, Vol. 45, No. 12, 601–602, 2009.
13. Habashi, J. Nourinia, and C. Ghobadi, "Mutual coupling reduction between very closely spaced patch antennas using low-profile folded split-ring resonators (FSRRs)," *IEEE Antennas Wireless Propag. Lett.*, Vol. 10, 862–865, 2011.
14. Gheethan, A. A., P. A. Herzig, and G. Mumcu, "Compact 2×2 coupled double loop GPS antenna array loaded with broadside coupled split ring resonators," *IEEE Trans. Antennas Propag.*, Vol. 61, No. 6, 3000–3008, 2013.
15. Yang, X. M., X. G. Liu, X. Y. Zhou, and T. J. Cui, "Reduction of mutual coupling between closely packed patch antennas using waveguided metamaterials," *IEEE Antennas Wireless Propag. Lett.*, Vol. 11, 389–391, 2012.
16. Li, Q., A. P. Feresidis, M. Mavridou, and P. S. Hall, "Miniaturized double-layer EBG structures for broadband mutual coupling reduction between UWB monopoles," *IEEE Trans. Antennas Propag.*, Vol. 63, No. 3, 1168–1171, 2015.
17. Qi, H. Y., L. L. Liu, X. X. Yin, H. X. Zhao, and W. J. Kulesza, "Mutual coupling suppression between two closely spaced microstrip antennas with an asymmetrical coplanar strip wall," *IEEE Antennas Wireless Propag. Lett.*, Vol. 15, 191–194, 2016.
18. Qi, H. Y., X. X. Yin, and H. X. Zhao, "A hybrid solution for mutual coupling reduction between closely spaced microstrip antennas," *2015 Asia-Pacific Microwave Conference*, Vol. 3, 1–3, 2015.
19. Park, C. H. and H. W. Son, "Mutual coupling reduction between closely spaced microstrip antennas by means of H-shaped conducting wall," *Electron. Lett.*, Vol. 52, No. 13, 1093–1094, 2016.
20. Hammoodi, A. I., H. M. Al-Rizzl, and A. A. Isaac, "Mutual coupling reduction between two monopole antennas using fractal based DGS," *IEEE Inter. Symp. on Antennas and Propag. and USNC/URSI National Radio Science Meeting*, 416–417, 2015.
21. Kakaoyiannis, C. G. and P. Constantinuo, "Reducing coupling in compact arrays for WSN nodes via pre-fractal defected ground structures," *Proceeding of the 39th European Microwave Conference*, Roma, Italy, 2009.
22. Kumar, N. and U. Kiran Kommuri, "MIMO antenna mutual coupling reduction for WLAN using spiro meander line UC-EBG," *Progress In Electromagnetics Research C*, Vol. 80, 65–77, 2018.